

Journal of Visualized Experiments

Transverse fracture of the mouse femur with stabilizing pin

--Manuscript Draft--

Article Type:	Invited Methods Collection - JoVE Produced Video
Manuscript Number:	JoVE63074R2
Full Title:	Transverse fracture of the mouse femur with stabilizing pin
Corresponding Author:	David Maridas UNITED STATES
Corresponding Author's Institution:	
Corresponding Author E-Mail:	david_maridas@hsdm.harvard.edu
Order of Authors:	David Maridas Emily Moore Marina Feigenson
Additional Information:	
Question	Response
Please specify the section of the submitted manuscript.	Biology
Please indicate whether this article will be Standard Access or Open Access.	Standard Access (\$1400)
Please indicate the city, state/province, and country where this article will be filmed . Please do not use abbreviations.	Boston, MA, USA
Please confirm that you have read and agree to the terms and conditions of the author license agreement that applies below:	I agree to the Author License Agreement
Please confirm that you have read and agree to the terms and conditions of the video release that applies below:	I agree to the Video Release
Please provide any comments to the journal here.	

TITLE:

Transverse Fracture of the Mouse Femur with Stabilizing Pin

AUTHORS AND AFFILIATIONS:

Emily R. Moore¹, Marina Feigenson², David E. Maridas^{1*}

¹Harvard School of Dental Medicine, Department of Developmental Biology, 188 Longwood Avenue, Boston, MA 02115, USA

²Keros Therapeutics, 99 Hayden Avenue, Suite 120, Building E, Lexington, MA 02421

Email addresses of the authors:

Emily R. Moore (emily_moore@hsdm.harvard.edu)

Marina Feigenson (Marina@kerostx.com)

David E. Maridas (david_maridas@hsdm.harvard.edu)

*Email address of the corresponding author:

David E. Maridas (david_maridas@hsdm.harvard.edu)

KEYWORDS:

Mouse, fracture, femur, bone, injury, periosteum

SUMMARY:

This protocol describes a method to perform fractures on adult mice and monitor the healing process.

ABSTRACT:

Fracture repair is an essential function of the skeleton that cannot be reliably modeled *in vitro*. A mouse injury model is an efficient approach to test whether a gene, gene product or drug influences bone repair because murine bones recapitulate the stages observed during human fracture healing. When a mouse or human breaks a bone, an inflammatory response is initiated, and the periosteum, a stem cell niche surrounding the bone itself, is activated and expands. Cells residing in the periosteum then differentiate to form a vascularized soft callus. The transition from the soft callus to a hard callus occurs as the recruited skeletal progenitor cells differentiate into mineralizing cells, and the bridging of the fractured ends results in the bone union. The mineralized callus then undergoes remodeling to restore the original shape and structure of the healed bone. Fracture healing has been studied in mice using various injury models. Still, the best way to recapitulate this entire biological process is to break through the cross-section of a long bone that encompasses both cortices. This protocol describes how a stabilized, transverse femur fracture can be safely performed to assess healing in adult mice. A surgical protocol including detailed harvesting and imaging techniques to characterize the different stages of fracture healing is also provided.

INTRODUCTION:

Fractures, breaks in the continuity of the bone surface, occur in all segments of the population.

They become severe in people who have fragile bones due to aging or disease, and the health care costs of fragility fractures are expected to exceed \$25 billion in 5 years¹⁻⁵. Understanding the biological mechanisms involved in fracture repair would be a starting point in developing new therapies aimed at enhancing the healing process. Previous research has shown that, upon fracture, four significant steps occur that enable bone to heal: (1) formation of the hematoma; (2) formation of a fibrocartilaginous callus; (3) mineralization of the soft callus to form bone; and (4) remodeling of the healed bone^{6,7}. Many biological processes are activated to heal the fracture successfully. First, an acute pro-inflammatory response is initiated immediately after a fracture^{6,7}. Then, the periosteum becomes activated and expands, and periosteal cells differentiate into chondrocytes to form a cartilage callus that grows to fill the gap left by the disrupted bone segments⁶⁻⁹. Neural and vascular cells invade the newly formed callus to provide additional cells and signaling molecules needed to facilitate repair⁶⁻¹⁰. In addition to contributing to callus formation, periosteal cells also differentiate into osteoblasts that lay down woven bone in the bridging callus. Finally, osteoclasts remodel the newly formed bone to return to its original shape and lamellar structure⁷⁻¹¹. Many groups developed mouse models of fracture repair. One of the earlier and most often used fracture models in mice is the Einhorn approach, where weight is dropped on the leg from a specific height¹². The lack of control over the angle and the force applied to induce the fracture creates a lot of variability in the location and size of the bone discontinuity. Subsequently, it results in variations in the specific fracture healing response observed. Other popular approaches are surgical intervention to produce a tibial monocortical defect or stress fractures, procedures that induce comparatively milder healing responses^{10,13}. Variability in these models is primarily due to the person conducting the procedure¹⁴.

Here, a detailed mouse femur injury model allows for control over the break to provide a reproducible injury and allow for quantitative and qualitative assessment of femur fracture repair. Specifically, a complete breakthrough in the femurs of adult mice is introduced and stabilizes the fracture ends to account for the role physical loading plays in bone healing. The methods for harvesting tissues and imaging the different steps of the healing process using histology and microcomputed tomography (microCT) are also provided in detail.

PROTOCOL:

All animal experiments described were approved by the Institutional Animal Care and Use Committee of the Harvard Medical Area. 12-week-old C57BL/6J mice (males and females) were used in this protocol. C57BL/6J male and female mice achieve peak bone mass around 12 weeks of age with femurs wide enough to fit a stabilizing pin, making them an appropriate strain to use for this protocol¹⁵.

1. Preparation for the surgery

1.1. Autoclave the surgical equipment, including surgical scissors, straight forceps, curved forceps, surgical clamps, and diamond cutting wheel (see **Table of Materials**) to minimize the risk of infection.

1.2. Place a clean mouse cage on a heating pad to facilitate post-surgical recovery. Set the

heat pad to reach a temperature between 37-45 °C.

1.3. Place the mouse under anesthesia using an isoflurane chamber. Set the induction oxygen flow at 2 L/min, the isoflurane induction at 2-4%, the maintenance nose cone oxygen at 2 L/min, and the maintenance isoflurane is 1.4%.

1.4. Confirm that the mouse's breathing is stable, and they do not respond to a toe pinch. Apply a thin layer of ophthalmic ointment on each eye to prevent corneal scratching. Transfer the mouse to a sterile pad and maintain anesthesia using a nose cone to deliver isoflurane continuously at the same rate as in step 1.3.

NOTE: Using 12-week-old mice or older is recommended as femurs from younger mice might be too thin to accommodate a stabilizing pin.

1.5. Inject the mouse subcutaneously with 0.05 mg/kg body weight of slow-release buprenorphine (see **Table of Materials**).

1.6. Using an electric trimmer, shave a 2 x 2 cm square on both thighs corresponding to the location of the femur.

1.7. Disinfect the shaved area using sterile gauze or swabs to spread a layer of iodine followed by a rinse with 70% ethanol (**Figure 1A**).

2. Surgery

2.1. Using a sterile scalpel, make a 5 mm incision in the shaved, disinfected region and peel away the skin to expose the underlying fascia.

2.2. Use straight forceps and fine scissors to delicately grab and cut the fascia directly, covering the femur to expose the muscle. A 5 mm cut of the fascia is sufficient to access the underlying muscle.

2.3. Using one pair of straight forceps, gently separate the muscle from the femur with minimal tissue damage.

2.4. Once the femur is visible, slide the curved forceps underneath the femur between the separated muscle and bone. Let the forceps slowly open to maintain muscle separation and secure the femur to facilitate a clean cut.

NOTE: The femur must stay exposed and separated from the muscle and skin when the forceps are not held, as shown in **Figure 1B**.

2.5. Make a transverse cut in the middle of the femur shaft using a handheld saw on the low power setting (See **Table of Materials** for the blade and Rotary Tool Kit used).

NOTE: Once the femur is completely cut, two fracture ends are created: the proximal section (attached to the hip bone) and the distal section (attached to the knee, also known as the stifle joint). Avoid cutting the femur in one single motion. Instead, make 3-5 passes until the femur is completely cut through. This is critical to avoid overheating the surrounding tissue and generating significant bone debris, negatively impacting healing.

2.6. Insert a guide needle (23 G x 1 TW IM, 0.6 mm x 25 mm) (see **Table of Materials**) in the marrow cavity of the distal section. Use fingers to gently twist the needle to push to thread through the knee joint (**Figure 1C**).

2.6.1. Remove the guide needle from the distal end and repeat on the proximal end, using the same gentle twisting motion to push the guide needle through the hip joint. Leave the guide needle in the proximal end, with its tip emerged from the skin (**Figure 1D**).

NOTE: To stabilize the fracture ends, a guide needle was first used to create a pathway through the fracture ends, and then a stabilizing pin was threaded through this pathway to secure the fracture ends¹⁴.

2.7. Insert the stabilizing pin (needle, 27 G x 1 ¼, 0.4 mm x 30 mm) (see **Table of Materials**) into the tip of the guide needle (**Figure 1E**). Gently push so that the stabilizing pin enters as the guide needle exits the marrow cavity of the proximal end.

2.7.1. Discard the guide needle. Use tweezers to hold and align the distal end with the proximal end and continue to thread the stabilizing pin through the distal marrow cavity until it exits the knee joint using the pathway made in 2.6 (**Figure 1F**).

NOTE: The stabilizing pin should now be protruding from the hip and the knee joints.

2.8. Using the surgical clamp, pull the tip of the pin to bring the proximal and distal sections close together, so they are barely touching. Realign the fracture ends with forceps if needed, and fold the ends of the stabilizing pin toward the fracture site using the surgical clamp (see **Table of Materials**).

2.8.1. Remove the plastic from the base of the needle using wire cutters. Using the clamp, twist both ends of the pin until they are blunt to avoid internal tissue damage.

NOTE: The fracture ends are now locked in place so that the mouse can put weight on the injured leg. The pin is secured if the fracture ends are unable to separate. A wire cutter can also be used to blunt the ends. The stabilizing pin must stay in place for the whole duration of the study until the mouse is euthanized. Attempts at dislodging the pin are likely to destabilize the fracture response and cause harm to the animal. The pin can be removed at dissection.

2.9. Use straight forceps to replace the muscle onto the femur. Using curved forceps, pinch

the ends of the skin together and close the opening using wound clips.

NOTE: Do not close the skin too tightly with the clips, or the mouse will avoid putting weight on this leg. Limiting physical loading during recovery could delay the healing process.

2.10. Repeat steps 2.2 to 2.4 on the other leg and close the wound without performing the femur fracture.

NOTE: This sham-operated femur serves as the contralateral control.

2.11. Withdraw the isoflurane exposure, place the mouse in the heated cage, and ensure they regain consciousness within 10-15 min.

2.12. Monitor the mouse's activity and incision site daily for the 5 days after surgery for signs of distress or infection.

NOTE: If the animal demonstrates signs of pain, is not eating, and/or hesitates to walk on their hindlimbs, consult with veterinary personnel and administer additional analgesic.

2.13. Remove the wound clips 10 days after the surgery.

NOTE: If the wound does not appear to have close after 10 days, consult the veterinary personnel and IACUC before removing the clips.

3. Tissue harvest

3.1. Euthanize the mice *via* CO₂ inhalation followed by cervical dislocation.

NOTE: This procedure is consistent with the Panel on Euthanasia of the American Veterinary Medical Association.

3.2. Using scissors and forceps, remove the skin from both mouse legs, dislocate the femoral head from the hip bone, and cut adjacent muscle to free the leg.

NOTE: Avoid removing too much muscle around the femur as the callus could be dislodged or damaged.

3.3. Avoiding the stabilizing pin, cut through the knee joint to separate the femur from the tibia.

3.4. Dissect around the distal and proximal parts of the femur to expose the ends of the stabilizing pin.

3.5. With a hard wire cutter, cut the folded blunt ends of the pin so only the straight portion

of the pin remains. Use forceps to slowly and gently slide the stabilizing pin out of the femur.

NOTE: If the pin does not easily slide out, do not apply force as this could dislodge the callus and damage the sample. Instead, try to rotate the pin and remove it delicately. Removal of the pin may also be easier after fixation.

4. Histology – Alcian Blue / Eosin /Orange G staining

NOTE: Alcian Blue/Orange G/Eosin staining is routinely used to visualize cartilage (blue) and the bone (pink). The cartilage area can be quantified as a proportion of the total callus area (**Figure 2A,B**).

4.1. Fix femurs in 10% neutral buffered formalin overnight at 4 °C.

4.2. Wash the fixed samples in phosphate-buffered saline (PBS).

4.3. Place samples in 0.5M EDTA, pH 8.0 on a slowly rotating shaker for 2 weeks. Change EDTA solution every other day to ensure efficient decalcification.

NOTE: No specific rpm is required for the shaker; ensure that the liquid flows in the container to cover all the samples. Complete decalcification can be tested by X-ray of the femurs.

4.4. To process the samples for paraffin embedding incubate them in the following solutions (1 h each): 70% EtOH, 95%EtOH, 100%EtOH, 100%EtOH, Xylene, Xylene, Paraffin, Paraffin.

4.5. Embed the samples in paraffin for sectioning.

4.6. Cut 5-7 µm thick longitudinal sections of the fractured femurs using a microtome.

4.7. Deparaffinize the sections by incubating them in 2 baths of Xylene (5 min each).

4.8. Rehydrate the sections by incubating the following ethanol gradient (2 min each): 100% EtOH, 100% EtOH, 80% EtOH, 70% EtOH.

4.9. Place slides in tap water for 1min.

4.10. Make the solutions of Alcian blue, Acid alcohol, Ammonium water, and Eosin/Orange G for histology as mentioned in **Supplementary File 1**.

NOTE: The suggested volumes of each solution should be sufficient to submerge the slides for the staining completely.

4.11. Place slides in Acid alcohol for 30 s and incubate in Alcian blue for 40 min.

- 265 4.12. Wash gently under the running tap until the water is clear for about 2 min.
266
267 4.13. Dip the slides rapidly in acid alcohol for 1 s.
268
269 4.14. Rinse as described in step 4.9.
270
271 4.15. Incubate in **ammonium water** for 15 s.
272
273 4.16. Rinse as described in step 4.9.
274
275 4.17. Place in 95% ethanol for 1 min and incubate in Eosin/Orange G for 90 s.
276
277 4.18. Dehydrate the slides quickly with a single dip in 70% EtOH, 80% EtOH and 100%EtOH.
278
279 4.19. Place slides in Xylene for 1 min to clear the slides.
280
281 4.20. Apply mounting media and a coverslip for imaging.
282

283 NOTE: For molecular analysis, RNA and protein can be isolated from the callus. Carefully dissect
284 the muscle under a dissecting scope and separate the callus from the underlying bone using a
285 scalpel.
286

287 5. **MicroCT**

288

289 NOTE: In the later stages of healing, microCT can be performed to image and quantify the
290 mineralization in the hard callus and the fracture gap. In C57BL/6J mice, the callus is usually
291 mineralized and detectable by microCT after 10 days post-fracture (dpf) (**Figure 2C**).
292

- 293 5.1. Fix femurs in 10% neutral buffered formalin overnight at 4 °C.
294

295 NOTE : MicroCT can be performed on the same femurs used for histology as long as it is done
296 before EDTA decalcification (step 4.3). When using the same femurs for both techniques, perform
297 micro CT, retrieve the samples and go to step 4.3.
298

- 299 5.2. Wash the fixed samples in phosphate-buffered saline (PBS) and store in 70% EtOH.
300

- 301 5.3. Perform MicroCT with an isotropic voxel size of 7 μm at an energy level of 55 kVP and an
302 intensity of 145 μA (see **Table of Materials**).
303

- 304 5.4. Contour the microCT slices to include the callus and exclude the cortical bone.
305

306 NOTE: As the callus gets more mineralized with time, the threshold can be adjusted to visualize
307 and measure the callus volume at different stages.
308

5.5. Obtain the bone volume contained in the callus contours as a measurement of the callus volume.

NOTE: Fracture gap can be measured directly on the microCT slices as the distance occupied by the break.

REPRESENTATIVE RESULTS:

In C57BL/6J mice, a successful surgery completes the protocol as mentioned earlier, healing steps in the fractured femur and little to no local inflammatory response or periosteal involvement in the sham-operated contralateral femur. A hematoma is formed a few hours after surgery, and the periosteum is activated to recruit skeletal progenitors for chondrogenesis. Various cell populations, such as Prx1⁺ mesenchymal progenitors, can be traced during the repair process using commercially available fluorescent reporter mouse models (**Figure 3**). Alcian Blue staining ~5 dpf can visualize the soft callus, and the cartilage area can be quantified (**Figure 2A,B**). Mineralization is detectable by microCT ~28 dpf (**Figure 2C**). The volume of the mineralized callus and mechanical testing to measure bone strength are commonly used as quantifiable outcomes of fracture repair. Genetic modification or drug intervention can change the course of recovery, so performing a time-course study to characterize fractures at different stages of repair is recommended. The whole callus can be dissected for molecular analysis, and the contralateral bone shaft can be used as a control. If the fracture ends are not aligned or adequately secured with the pin, the resulting images will show a lack of callus formation on all or one side of the fracture end of the fracture (**Figure 4**).

FIGURE LEGENDS:

Figure 1: Fracture and insertion of the stabilizing pin. (A) A square is shaved on the right leg of a C57BL/6J mouse. (B) After an incision is made to the skin and fascia, curved forceps are secured underneath the femur to separate the muscle, skin, and bone. (C) After the cut is made, two fracture ends are created: the proximal section of the femur attached to the hip bone and the distal section attached to the knee. The guide needle (green) is inserted into the distal section and pushed through the knee joint. (D) The guide needle is removed from the distal section, inserted in the proximal section, and pushed through the hip joint. (E) The stabilizing pin (grey needle) is inserted into the guide needle protruding from the hip joint. (F) The stabilizing pin is pushed through the proximal section, into the distal section, and through the knee joint using the path made by the guide needle in C.

Figure 2: Histology and microCT of femur fracture. (A) Formalin-fixed paraffin sections of femur fractures were collected at 5, 10, and 28 dpf and stained with Alcian Blue/Eosin/Orange G. Scale bar = 500 μ m. (B) Cartilage area was quantified using ImageJ software at 5, 10, and 28 dpf. (C) At 28 dpf, mineralization was observed, and the callus volume and fracture gap could be measured by microCT. Scale bar = 1,000 μ m. Data shown as Mean \pm SEM. The mineralized callus volume was measured by contouring around the cortical bone at the fracture site. The dark grey area delineates the mineralized callus on the image, while the cortical bone (light grey) is not included in the measurement. Data shown as Mean \pm SEM.

Figure 3: Fluorescent reporter model used to visualize expansion of Prx1⁺ periosteal cells after fracture. Prx1CreER; Rosa26^{tdTomato} mice were injected daily for five days with 80 mg/kg body weight of tamoxifen to induce tdTomato expression. Three days after the final injection, femur fracture was initiated, and mice were sacrificed at 7 or 14 dpf to track where Prx1-expressing cells and their progeny (Prx1⁺) are located within the fracture callus and expanded periosteum. Scale bar = 500 μ m.

Figure 4: Example of irregular healing due to surgical issues. Fracture ends were not aligned properly and the stabilizing pin pierced through the proximal section of the femur in this example. These errors resulted in callus formation where the femur was pierced rather than (yellow box) at the cut site. Scale bar = 500 μ m.

Supplementary File 1: Composition of the solutions required for histology.

DISCUSSION:

The injury model detailed in this protocol encompasses all the four significant steps observed during the healing of spontaneous fractures, including (1) pro-inflammatory response with the formation of the hematoma; (2) recruitment of skeletal progenitors from the periosteum to form the soft callus, (3) mineralization of the callus by osteoblasts and (4) remodeling of the bone by osteoclasts.

The surgical procedure described in this manuscript is optimized for adult mice at least 12 weeks old. A 27 G x 1 $\frac{1}{4}$ (0.4 mm x 30 mm) needle is used as the stabilizing pin because it is the ideal size for the width of the marrow cavity at this age. If needed, the protocol could be amended for younger animals if a thinner stabilizing pin is used. The stabilizing pin is an essential part of the surgery's success as it was demonstrated that instability significantly affects fracture healing¹⁶. Other stabilization methods have been reviewed, and all come with their advantages and limitations¹⁷⁻¹⁹. The ideal stabilization should be selected based on the research question and experimental goal. One limitation of the described stabilization here is that the pin goes through the cartilage and knee and hip joints. If the contribution from the articular or growth plate cartilage is of concern, we suggest considering another stabilizing method.

Variability in surgical technique and between animals is a concern when performing this surgery. Therefore, it is recommended to use ample numbers, especially for quantitative readouts, and to compare similar types of fractures across groups. It is critical to secure the femur sections close together to avoid gaps over 2 mm. Variability in gaps between sections can considerably affect the size of the callus and the timing of repair. The sections should also be properly aligned. Loose and misaligned fractures will cause more significant variability across samples and might impair healing.

Weight-bearing is also crucial for the timing of bone healing and can introduce variability between mice. Most mice put minimal weight on the injured leg a few hours after surgery but should normally walk by the next day. Verifying that the mouse moves normally and the load is

distributed evenly on both legs is crucial, especially when using the contralateral femur as a sham-operated control. In addition, the surgery can trigger a systemic inflammation that affects the contralateral leg. It is therefore recommended to compare sham-operated femurs to non-operated mice when establishing this technique. Having non-operated controls could also be preferable for quantifiable outcomes such as effects on RNA or protein expression.

Consistency of the fracture geometry can be challenging with other methods²⁰, using a saw allows for more control for the surgeon and alleviates the variability in ensuing fractures. The saw approach has also been used to create metaphyseal fractures of the proximal mouse femurs successfully²¹.

Differences between male and female mice in their response to fracture healing are rarely observed. However, sex may become a factor with age and drug intervention, so comparing animals of the same sex or performing statistics to interrogate sex differences before combining samples is strongly recommended. Furthermore, this protocol was designed for C57BL6/J mice. Investigators using other mouse strains should confirm the appropriate age to achieve peak bone mass and a large femoral marrow cavity for the guide needle.

We believe this femur fracture surgery is an efficient model to recapitulate the significant healing steps in mice and can be used to test the effects of genetic modifications or therapeutic interventions on fracture recovery in humans.

ACKNOWLEDGMENTS:

We thank Dr. Vicki Rosen for financial support and guidance with the project. We would also like to thank the veterinary and IACUC staff at the Harvard School of Medicine for consultation regarding sterile technique, animal well-being, and the materials used to develop this protocol.

DISCLOSURES:

The authors do not have any conflicts of interest to disclose.

REFERENCES:

1. Black, D. M., Rosen, C. J. Postmenopausal osteoporosis. *The New England Journal of Medicine*. **374**, 2096-2097 (2016).
2. Curtis, E. M., Moon, R. J., Harvey, N. C., Cooper, C. The impact of fragility fracture and approaches to osteoporosis risk assessment worldwide. *Bone*. **104**, 29-38 (2017).
3. Laurent, M. R., Dedeyne, L., Dupont, J., Mellaerts, B., Dejaeger, M., Gielen, E. Age-related bone loss and sarcopenia in men. *Maturitas*. **122**, 51-56 (2019).
4. NOF. *National Osteoporosis Foundation - Just for men*, <https://cdn.nof.org/wp-content/uploads/2015/12/Osteoporosis-Fast-Facts.pdf> > (2019).
5. Williams, S. A. et al. Economic burden of osteoporotic fractures in US managed care enrollees. *The American Journal of Managed Care*. **26**, e142-e149 (2020).
6. Sheen, J. R., Garla, V. V. Fracture healing overview. *StatPearls*. <https://www.ncbi.nlm.nih.gov/books/NBK551678/> (2021).
7. Holmes, D. Closing the gap. *Nature*. **550**, S194-S195 (2017).
8. Duchamp de Lageneste, O. et al. Periosteum contains skeletal stem cells with high bone

regenerative potential controlled by Periostin. *Nature Communications*. **9**, 773 (2018).

9. Bahney, C. S. et al. Cellular biology of fracture healing. *Journal of Orthopaedic Research*. **37**, 35-50 (2019).

10. Li, Z. et al. Fracture repair requires TrkA signaling by skeletal sensory nerves. *Journal of Clinical Investigation*. **129**, 5137-5150 (2019).

11. Colnot, C., Thompson, Z., Miclau, T., Werb, Z., Helms, J. A. Altered fracture repair in the absence of MMP9. *Development*. **130**, 4123-4133 (2003).

12. Bonnarens, F., Einhorn, T. A. Production of a standard closed fracture in laboratory animal bone. *Journal of Orthopaedic Research*. **2**, 97-101 (1984).

13. Hu, K., Olsen, B. R. Osteoblast-derived VEGF regulates osteoblast differentiation and bone formation during bone repair. *Journal of Clinical Investigation*. **126**, 509-526 (2016).

14. Collier, C. D. et al. Characterization of a reproducible model of fracture healing in mice using an open femoral osteotomy. *Bone Reports*. **12**, 100250 (2020).

15. Glatt, V., Canalis, E., Stadmeier, L., Bouxsein, M. L. Age-related changes in trabecular architecture differ in female and male C57BL/6J mice. *Journal of Bone and Mineral Research*. **22**, 1197-1207 (2007).

16. Garcia, P. et al. A new technique for internal fixation of femoral fractures in mice: impact of stability on fracture healing. *Journal of Biomechanics*. **41**, 1689-1696 (2008).

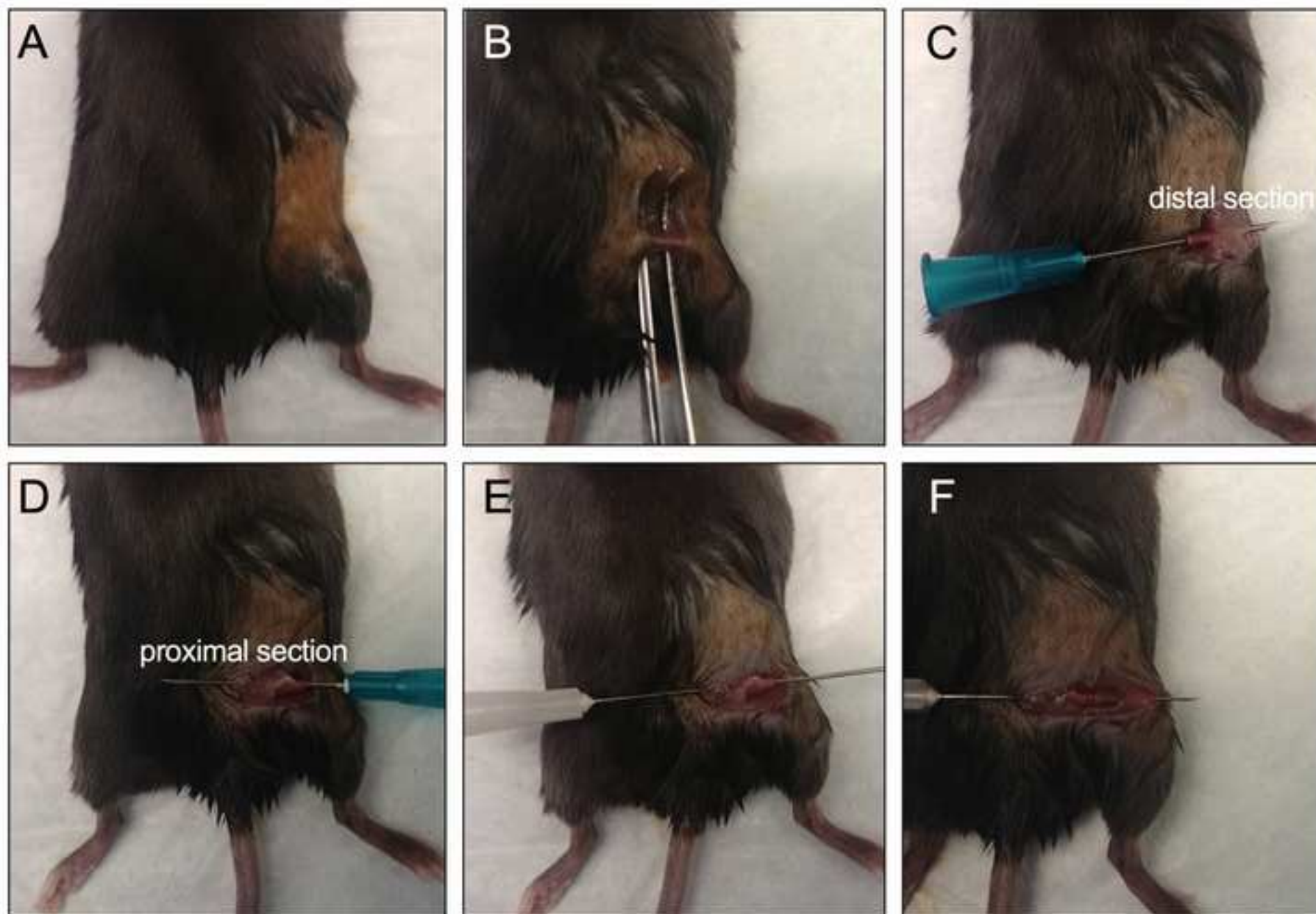
17. Holstein, J. H. et al. Advances in the establishment of defined mouse models for the study of fracture healing and bone regeneration. *Journal of Orthopaedic Trauma*. **23**, S31-38 (2009).

18. Garcia, P. et al. Rodent animal models of delayed bone healing and non-union formation: a comprehensive review. *European Cells & Materials*. **26** (1-12), discussion 12-14 (2013).

19. Histing, T. et al. Ex vivo analysis of rotational stiffness of different osteosynthesis techniques in mouse femur fracture. *Journal of Orthopaedic Research*. **27**, 1152-1156 (2009).

20. Williams, J. N., Li, Y., Valiya Kambrath, A., Sankar, U. The Generation of closed femoral fractures in mice: A model to study bone healing. *Journal of Visualized Experiments*. **138**, e58122 (2018).

21. Haffner-Luntzer, M. et al. A novel mouse model to study fracture healing of the proximal femur. *Journal of Orthopaedic Research*. **38**, 2131-2138 (2020).



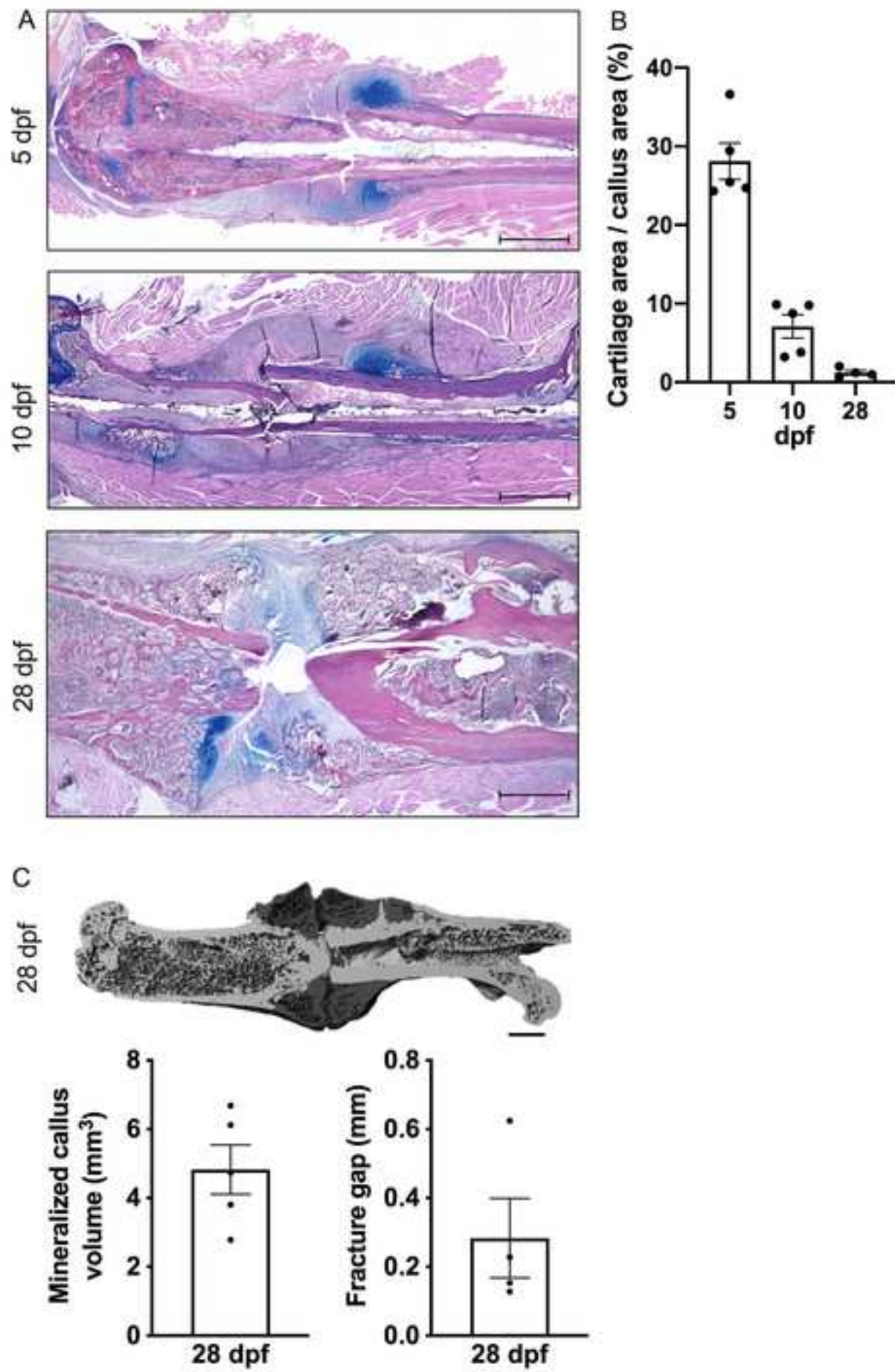


Figure 3

[Click here to access/download;Figure;Figure 3.tiff](#) 

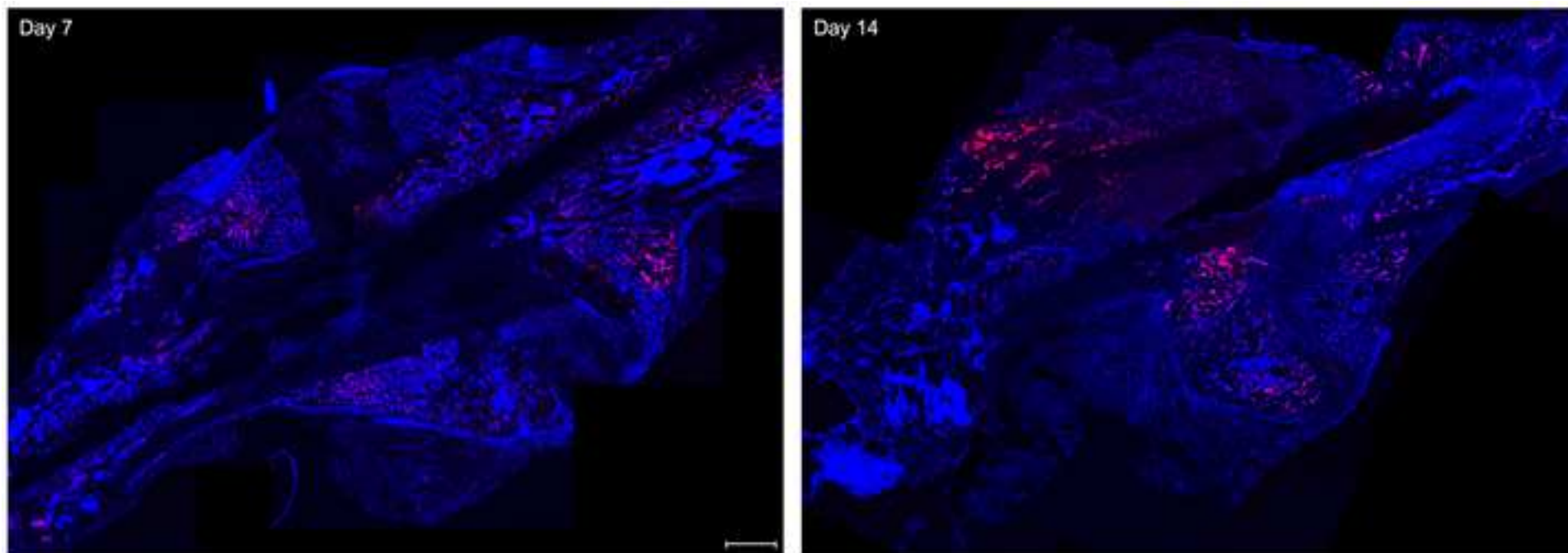
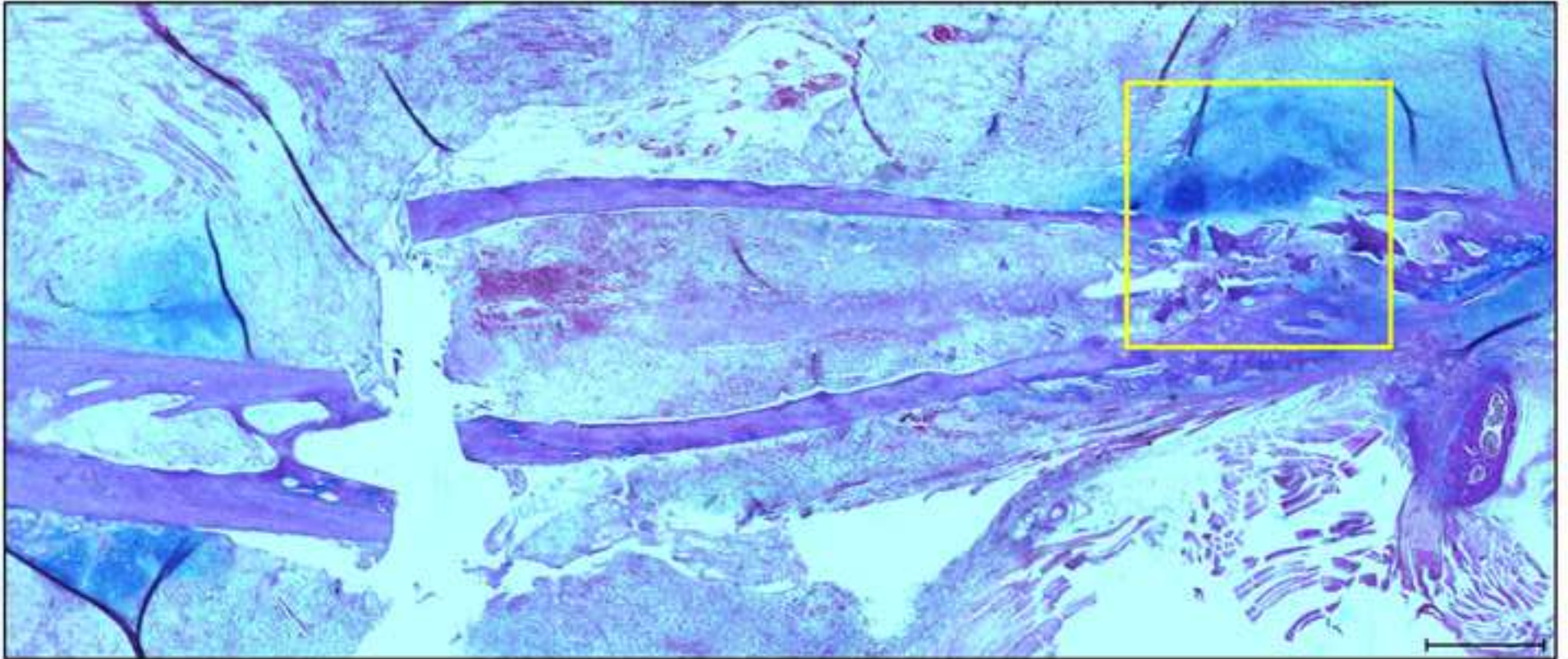


Figure 4

[Click here to access/download;Figure;Figure 4.tiff](#) 





[Click here to access/download](#)

Table of Materials
63074_R2_Table of Materials.xlsx





HARVARD

School of Dental Medicine

September, 13th 2021

RE: Manuscript resubmission – Rebuttal letter

Dear Amit,

We are pleased to resubmit our revised manuscript to the *Journal of Visualized Experiments*. We have comprehensively edited the article to address all the editorial comments. We also carefully addressed all the insightful comments of the reviewers point by point (below).

We decided to add a lot more details in the protocol description as well as new quantification measurements for fracture assessment. With the input from the editor and the reviewers, we believe our manuscript is stronger and ready for submission.

Thank you for your consideration.

Best,
David Maridas, PhD.

Point by point rebuttal:

Reviewer #1:

Manuscript Summary:

In this protocol manuscript Maridas et al. provide a guide to performing fracture models in mice. The protocol is complete and clearly described, displaying the authors' noted expertise in this procedure. Publication of this method will be of great interest given that this is a commonly employed experimental model for bone biology and that there is still considerable variability in how experimental fractures are created and analyzed in mice. A few optional minor suggestions are offered for consideration below.

Major Concerns:
None

Minor Concerns:

1. This reviewer has observed several publications by various groups where radiographs show that the stabilizing pin projects into the stifle joint, presumably impairing mouse ambulation or causing undesirable secondary osteoarthritis. We find that it is necessary to take a needle or second stabilizing pin and push on the distal end of the stabilizing pin so that the distal end of the pin is fully beneath the articular cartilage surface. Is it correct that the method performed here does have the stabilizing pin initially protruding into the stifle joint, and the stabilizing pin is then trimmed back with clippers to minimize the degree to which it protrudes into the stifle joint? If so, a note that makes it explicit that the stabilizing pin cannot project into the stifle joint and may need to be carefully pushed into the bone further so that the distal end is beneath the cartilage surface will be helpful for many readers just starting with this procedure.

The reviewer made an important point about the stabilizing pin. We added a note in the protocol to clarify that the pin was going through the cartilage and the joints. We also added a paragraph in the discussion mentioning the limitations of having the pin damaging the cartilage and joint structures (Discussion paragraph).

2. A little bit of extra detail regarding how the guide needle and stabilizing pin are introduced into the femur would likely be helpful. In the version of the fracture procedure used here is the stabilizing pin also inserted percutaneously over the guide needle? Is the guide needle left in place or removed? A little bit more detail in this area may help clarity.

We would like to thank the reviewer to help us clarify the procedure of inserting the stabilizing pin. We added extensive details to the steps in the protocol to illustrate the way the guide needle is used and

the stabilizing pin is introduced and we made sure to clarify that the guide needle is removed (steps 2.6 and 2.7). We also added those steps in Figure 1.

3. It may be helpful to mention in passing that the knee in mice is formally termed the stifle joint.

To address this comment, we mentioned that the knee is also known as the stifle joint in the protocol (Step 2.5).

4. For some studies, especially those studying fracture related immune responses/osteoimmunology, the use of the contralateral side as a mock fracture control may not be desirable, as fracture related inflammation may have systemic effects impacting bone. Similarly, secondary biomechanical compensation to the fracture may change the biology of the contralateral leg. It may be helpful to add a brief note that encourages readers to think about these issues and carefully consider whether contralateral controls versus a separate mouse undergoing a sham fracture operation is most appropriate for their study.

This is an excellent point made the reviewer. We added a paragraph in the discussion of the manuscript explaining the limitation of the use of the contralateral sham operation as a control. We think this would ensure that readers are carefully considering the proper controls for their experiments (Discussion paragraph).

5. This reviewer also sees a lot of confusion and inconsistency in the field about how to perform uCT endpoints for fracture. The approach taken in the example figure of uCT analysis offered here seems very good, and it may be helpful to elaborate a little bit further on this to help guide groups implementing this model for the first time to perform appropriate uCT analysis. This could include a little more detail on how the contouring is performed to identify just callus tissue and not underlying cortical bone, how thresholds may need to be adjusted to capture this newly formed bone that may be less radiopaque than the mature bone present since birth, and how among the many parameters available, the absolute volume of bone formed in the callus is a straightforward measure of healing, exactly as performed in the sample data image and graph provided here.

We would like to thank the reviewer for this comment and their appreciation of our μ CT.

We included a lot more details in the figure legend (Figure 3) about the specifics of the μ CT scan and measurement contouring. We also discussed adjusting the threshold at different stages of fracture healing as mineralization increases over time (Step 3.6).

Reviewer #2:

Manuscript Summary:

The manuscript "Transverse fracture of the mouse femur with stabilizing pin" by Maridas et al presents a protocol in which a femur fracture is induced in mice using an intramedullary nail, a method which can be used to study different biochemical, biomedical and biomechanical influences on fracture repair and which is therefore relevant to the field.

Major Concerns:

1) In the beginning of the discussion, fragility fractures are mentioned. This is an important point of interest within trauma surgery research. However, these fractures are also age related. From previous studies (Goodship et al), that the mouse strain which is used has a major influence on these factors. Which mouse strain is used in this protocol, and why?

The reviewer points out an important detail that was lacking in our previous manuscript. We added the strain and age of the mouse we are using in this protocol and the reason as to why in the first paragraph of the protocol.

2) In the surgical preparation paragraph, the optimal concentrations of isoflurane during induction and during inhalation anaesthesia (also including the flow of the gas) is not mentioned. Please specify.

The reviewer identified a critical detail missing in our protocol. We added all the information about the flow of oxygen and isoflurane in Step 1.3.

Minor Concerns:

1) How long can the intramedullary pin remain in situ?

This is a good question raised by the reviewer and points out a detail that was previously missing in our protocol. We specified that for this technique the pin must never be removed in situ (Step 2.8).

2) Line 170 mentions "control mice". How is this defined as there are no experimental groups to be found in this manuscript?

This is a good point made the reviewer. In our previous manuscript, it was unclear if we meant a non-operated control or another type of control mouse. We initially meant a "wild type" mouse, so we replaced the term "control" with "C57BL/6J" (Representative results section).

3) A lot of reviews comparing different fracture fixation techniques and their respective advantages and disadvantages have been published (Garcia, Holstein, Histing etc). This information would be of interest in the discussion of this manuscript.

We would like to thank the reviewer for raising this point. We also agree that the information published in those articles is of great use for readers trying to figure out the best surgical design to address their research question. We included those citations in our discussion paragraph and explained that other methods are available. We also detailed the main limitation of our fixation method to help the reader make the best decision for their experiment.

Solutions for histology:

Alcian Blue: Dissolve 1 g of Alcian Blue in 100 mL of Hematoxylin

Acid Alcohol: Mix 5 mL of hydrochloric acid with 495 mL of 70% ethanol

Ammonium water: Mix 2.5 g of ammonium hydroxide with 497.5 mL of water

Eosin / Orange G: Combine 34 mL of 1% Phloxine B, 16 mL of 2% Orange G, 450 mL of Eosin Y